Developmental Cell, Vol. 8, 689–701, May, 2005, Copyright ©2005 by Elsevier Inc. DOI 10.1016/j.devcel.2005.02.011

FGF Signal Interpretation Is Directed by Sprouty and Spred Proteins during Mesoderm Formation

Jeremy M. Sivak,[1,3] Lars F. Petersen,[1,2,3] and Enrique Amaya[1,2,*]

[1]The Wellcome Trust/Cancer Research UK Gurdon Institute
University of Cambridge
Tennis Court Road Cambridge
CB2 1QN
United Kingdom

[2]Department of Zoology
University of Cambridge
Downing Site, Cambridge
United Kingdom

Summary

Vertebrate gastrulation requires coordination of mesoderm specification with morphogenetic movements. While both of these processes require FGF signaling, it is not known how mesoderm specification and cell movements are coordinated during gastrulation. The related Sprouty and Spred protein families are recently discovered regulators of receptor tyrosine kinase signaling. We identified two genes for each family in *Xenopus tropicalis*: *Xtsprouty1*, *Xtsprouty2*, *Xtspred1,* and *Xtspred2*. In gain- and loss-of-function experiments we show that XtSprouty and XtSpred proteins modulate different signaling pathways downstream of the FGF receptor (FGFR), and consequently different developmental processes. Notably, XtSproutys inhibit morphogenesis and Ca^{2+} and PKCδ signaling, leaving MAPK activation and mesoderm specification intact. In contrast, XtSpreds inhibit MAPK activation and mesoderm specification, with little effect on Ca^{2+} or PKCδ signaling. These differences, combined with the timing of their developmental expression, suggest a mechanism to switch FGFR signal interpretation to coordinate mesoderm formation and cell movements during gastrulation.

Introduction

The formation and patterning of mesoderm represents a critical stage of vertebrate development. During gastrulation, mesodermal tissue must be coordinately induced and directed through a series of morphogenetic movements inside the embryo to form derivatives, such as muscle, notochord, and blood. Completion of these events is dependent on appropriate cellular responses to signals from a relatively small number of growth factors, including members of the fibroblast growth factor family (FGFs) (Sivak and Amaya, 2004).

We have shown previously that disrupting FGF receptor (FGFR) signaling inhibits mesoderm induction and maintenance (Amaya et al., 1991; Kroll and Amaya, 1996). The prominent pathway downstream of the FGFR during this process is the ras/MAPK pathway (Schlessinger, 2000). Inhibition of any component of this pathway subsequently blocks the expression of mesodermal markers (Gupta and Mayer, 1998; MacNicol et al., 1993; Tang et al., 1995; Whitman and Melton, 1992). FGF signaling has also been shown to directly affect morphogenetic cell movements during gastrulation (Ciruna et al., 1997; Yang et al., 2002). We have shown that this effect occurs through the FGFR via a mechanism that is distinct from the ras/MAPK pathway (Nutt et al., 2001). Therefore, FGFR signaling is used both for maintaining mesoderm fate and for regulating morphogenesis. However, how does the embryo interpret the signals correctly so that mesoderm maintenance and morphogenesis occur in a coordinated fashion?

We have previously reported that the receptor tyrosine kinase (RTK) inhibitor protein, Xsprouty2, inhibits FGFR- mediated morphogenesis but leaves mesoderm formation intact (Nutt et al., 2001). The Sprouty family was first discovered from a *Drosophila* mutation that mimicked the effects of overactive FGF signaling (Hacohen et al., 1998). A family of conserved Sprouty genes have since been identified that act as intracellular inhibitors of RTK signaling, with homologs found in mice, humans, zebrafish, and *Xenopus* (Christofori, 2003; Guy et al., 2003). Sprouty family members share a conserved cysteine-rich carboxy-terminal domain (Spry) and divergent amino termini (Guy et al., 2003). Recently, a Sprouty-related family, the Spreds, has also been described; they have been shown to inhibit RTK signaling as well. Spreds share the Spry domain but contain an N-terminal Enabled/VASP homology 1 domain (EVH1), and most have a binding sequence for the oncogenic RTK c-kit (Kato et al., 2003; Wakioka et al., 2001).

The biological roles of Sprouty and Spred proteins remain unclear due to results suggesting they have a variety of effects on RTK signaling. The majority of attention has focused on inhibition of MAPK activation by Sprouty proteins downstream of RTK signaling (Casci et al., 1999; Hanafusa et al., 2002). However, Sprouty family members have been shown to have variable effects on MAPK activation and even enhance MAPK signaling (Sasaki et al., 2001; Wong et al., 2002; Yusoff et al., 2002). We have shown that Xsprouty2 effectively inhibits Ca^{2+} signaling but has little effect on MAPK activation in vivo (Nutt et al., 2001). The Spreds also inhibit MAPK activity and have been reported to block activation of Raf (Kato et al., 2003; Wakioka et al., 2001). Notably, mammalian Spreds have been observed to be more potent inhibitors of MAPK activity than Sproutys in vitro (Wakioka et al., 2001).

Here we have identified two members of each the Sprouty and Spred families in the diploid frog *Xenopus tropicalis*: *Xtsprouty1* and *Xtsprouty2* and *Xtspred1* and *Xtspred2*. Using both gain- and loss-of-function experiments, we show that these two families of proteins help modulate FGF signal interpretation in the early embryo by inhibiting distinct downstream signal transduction

*Correspondence: ea3@mole.bio.cam.ac.uk

[3]These authors contributed equally to this work.

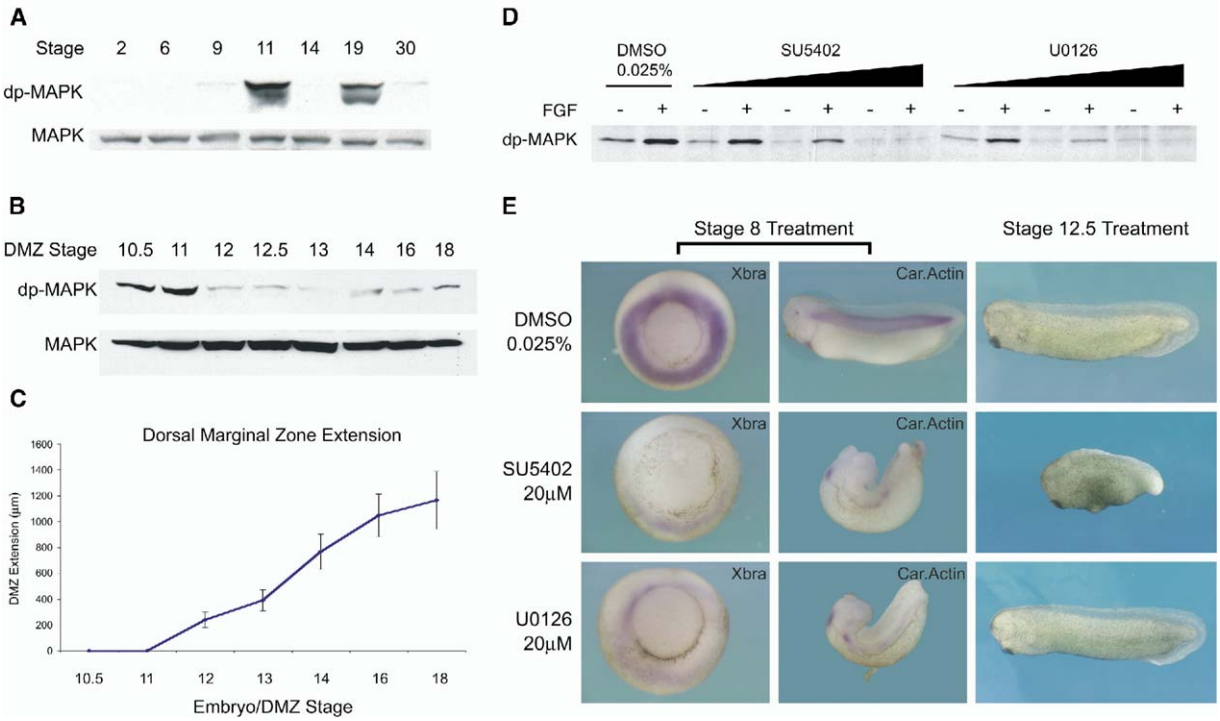

Figure 1. Morphogenesis Requires FGFR Signaling Independent of MAPK

(A) Western blots against embryo lysates from various stages probed for active MAPK (dp-MAPK) and pan-MAPK. MAPK activity peaked at stage 11 and decreased by stage 14, and then returned at stage 19.

(B) Blots for dp-MAPK and pan-MAPK against DMZ lysates at corresponding stages. Again, MAPK activity peaked at stage 11 and decreased sharply at stage 12, remaining low until stage 18.

(C) DMZ extension (μm) plotted against the corresponding stage. The majority of extension occurred between stages 12–16. Error bars represent standard deviation.

(D) dp-MAPK blots from animal cap lysates incubated for 15 min with and without FGF2 in the presence of increasing concentrations of FGFR1 inhibitor (SU5402) or MEK1 inhibitor (U0126). Both drugs abolished FGF-induced MAPK activation in a dosage-dependent manner.

(E) Embryos injected with 10 nl of 2 mM SU5402, U0126, or DMSO into the blastocell and cultured with the same inhibitor at stage 8 or 12.5. Stage 8 treated embryos were fixed at stage 11.5 and 29–30 for in situ hybridization for *Xbra* and *cardiac actin*, respectively. Both inhibitors blocked mesoderm specification and gastrulation movements when treated at stage 8. Embryos treated at stage 12.5 with SU5402 exhibited morphogenetic defects, but U0126-treated were unaffected.

pathways and thereby help coordinate mesoderm specification and morphogenesis.

Results

FGFR Signaling Is Required for Morphogenesis but Is Not Dependent on MAPK Activity

We have previously shown that Xsprouty2 inhibits FGF-dependent morphogenesis but does not affect mesoderm specification or MAPK activity in vivo. However, the role of MAPK signaling during morphogenesis has remained unclear. We therefore conducted a series of experiments to directly test the requirements of MAPK activation for morphogenetic movements during mesoderm formation.

First we determined the temporal profile of activated MAPK during the stages when morphogenetic movements are active during development, using antibodies specific for activated MAPK (dp-MAPK). We found that MAPK was active at stage 11 during mesoderm specification, but activity decreased by stage 14, after mesoderm had formed, and remained low until the late neurula stages (Figure 1A). In order to determine whether MAPK was active in the tissues undergoing active morphogenesis, we assayed MAPK activity in dissected dorsal marginal zone (DMZ) explants. Consistent with results from whole embryos, MAPK activity peaked in stage 11 DMZs and decreased by stage 12, where it remained low until stage 18 (Figure 1B). Notably, during the stages when MAPK activity was low we found that the DMZs were most actively undergoing morphogenesis (Figure 1C), suggesting that MAPK signaling is not required for this process.

To determine whether FGFR signaling is necessary for morphogenesis independently of MAPK, we used chemical inhibitors of the FGF receptor (SU5402) and MEK1 (U01236) to disrupt all FGFR activity or just MAPK activation, respectively. Both SU5402 and U0126 successfully inhibited FGF-stimulated MAPK activation in animal caps in a dose-dependent manner (Figure 1D). Embryos were then treated with SU5402, U0126, or DMSO control at stage 8 (before mesoderm specification) and stage 12.5 (after mesoderm specification, but prior to the stages of most extensive morphogenesis). Embryos exposed to either SU5402 or U0126 at stage 8 failed to complete gastrulation, resulting in an

open blastopore phenotype with decreased expression of mesodermal markers *Xbrachyury* (*Xbra*) and *cardiac actin* (Figure 1E) (percentage of open blastopore phenotypes: 0% [n = 48] in DMSO; 76.6% [n = 47] in SU5402; 84.4% [n = 45] in U0126)]. These results are consistent with the effects of disrupting the FGFR or ras/MAPK pathway during early stages of development. In comparison, embryos treated with the FGFR inhibitor (SU5402) at stage 12.5 showed morphogenetic defects resulting in a shortened anterior-posterior (A-P) axis, whereas embryos treated with the MAPK inhibitor (U0126) developed normally (Figure 1E) (percentage shorter than 4.5 mm at stage 29–30: 0% [n = 40] in DMSO; 92.3% [n = 29] in SU5402; 2.5% [n = 40] in U0126). Taken together, these results show that FGFR signaling is required for both mesoderm specification and morphogenesis, but only mesoderm specification depends on MAPK activity, suggesting that morphogenesis involves an alternate downstream pathway.

Xtsproutys and *Xtspreds* Are Related Families of FGFR Regulatory Genes that Share Overlapping Expression Patterns, but at Slightly Different Times

Based on our previous work, we hypothesized that Sprouty family members may be involved in regulating FGFR signal interpretation during development. We isolated two *X. tropicalis sprouty* genes, *Xtsprouty1* (*Xtspry1*) and *Xtsprouty2* (*Xtspry2*), and two related *spred* genes, *Xtspred1* (*Xtsprd1*) and *Xtspred2* (*Xtsprd2*). As with their mammalian counterparts, all the identified XtSprouty and XtSpred proteins share a conserved cysteine-rich C-terminal Spry domain. The two Sprouty proteins contain an uncharacterized N-terminal domain whose function remains obscure (Guy et al., 2003), while the two Spreds contain an N-terminal EVH1 domain and c-Kit binding domain (KBD) (Harmer et al., 2005; Wakioka et al., 2001) (Figure 2A). All proteins contain a high degree of identity to their human counterparts: 72.9% for Sprouty1, 72.7% for Sprouty2, 60.1% for Spred1, and 69.9% for Spred2.

The *Xtsprouty* and *Xtspred* genes are all expressed in broadly similar patterns to *X. laevis sprouty2* and a number of FGFs, including XFGF8, XeFGF, and FGF-9 (Christen and Slack, 1997; Isaacs et al., 1994; Nutt et al., 2001; Song and Slack, 1996). During gastrula stages, expression was first localized to the dorsal marginal zone, but later expanded laterally and ventrally. Although all four genes displayed this pattern, *Xtspry1* and *Xtspry2* were detected earlier and expanded their expression pattern more quickly than *Xtsprd1* and *Xtsprd2* (Figure 2B). During neurula stages, expression became confined anteriorly and posteriorly and expanded to varying degrees along the neural tube. Generally, staining for *Xtsproutys* became weaker and more localized, while *Xtspreds* became stronger and more broad. At tail bud stages, staining became localized to the developing branchial arches, forebrain, otic vesicle, midbrain/hindbrain isthmus, and tail bud. *Xtspry2* staining was absent from the third branchial arch; however, this feature was stained for *Xtspry1*, *Xtsprd1*, and *Xtsprd2* mRNAs. Comparatively, *Xtspred* gene expression overlapped considerably with the *Xtsprouty* genes, with the exception that staining for the *Xtspred* genes was either weak or absent in the midbrain/hindbrain isthmus and forebrain and did not extend as far posteriorly in the tail bud.

We next decided to determine whether the *Xtsprouty* and *Xtspred* genes are expressed at the same relative times. Since in situ hybridization data are not quantitative, we decided to answer this question using quantitative real-time RT-PCR. We found that, although the *Xtsprouty* and *Xtspred* genes share similar spatial patterns, they have important temporal differences. The relative expression levels by real-time RT-PCR of *Xtspry1* and *Xtspry2* was higher during early gastrula stages and then decreased, while *Xtsprd1* and *Xtsprd2* remained low during the early gastrula stages but increased significantly from the end of gastrulation through neurula stages (Figure 2C).

XtSprouty and XtSpred Gain-of-Function Experiments Cause Distinct Phenotypes

To begin to address the function of these genes, we injected in vitro transcribed mRNAs corresponding to the *Xtsprouty* and *Xtspred* genes into the dorsal marginal zones of *X. laevis* embryos at the two-cell stage. Embryos injected with *Xtsproutys* developed a shortened A-P axis, compared to controls injected with a nonfunctional FGF receptor (HAV∅) or uninjected embryos (Figures 3A and 3B). Interestingly, this phenotype is similar to that caused by treatment with an FGFR inhibitor at stage 12.5 (Figure 1E). In comparison, embryos injected with *Xtspreds* developed an open blastopore phenotype reminiscent of the effects of early FGFR inhibition (Figure 1E). These results prompted further investigations to determine if the differences between the *Xtsproutys* and *Xtspreds* were variations in severity of the same phenotype or caused by distinct underlying molecular mechanisms.

XtSpreds Inhibit Mesoderm Specification but XtSproutys Do Not

Early disruption of FGFR function blocks specification of mesoderm as well as failure to complete gastrulation. This effect is due to interruption of the MAPK signaling cascade controlling transcriptional activation of mesodermal genes, such as the T-box transcription factor *Xbrachyury* (*Xbra*) (Sivak and Amaya, 2004). We tested the effects of *Xtsprouty* and *Xtspred* overexpression on mesoderm specification and MAPK activity. A series of in situ hybridizations was carried out for *Xbra* on mid-gastrula embryos that had been coinjected with either *Xtsprouty* or *Xtspred*, and β-gal RNAs into one blastomere at the two-cell stage. Control-injected embryos showed a characteristic ring of *Xbra* expression in the marginal zone around the blastopore. Injections of either *Xtsprouty* had little effect on *Xbra*; however, both *Xtspreds* completely blocked *Xbra* expression on the injected side (Figure 3C).

We then assayed the effects of XtSprouty and XtSpred proteins on MAPK activity, using the dp-MAPK antibody. As shown previously, during gastrulation there is a sharp FGF-dependent increase in the amount of activated MAPK, concomitant with mesoderm specification (Figure 1A). When 1.0 ng RNAs was injected into both blastomeres, neither XtSprouty had an effect

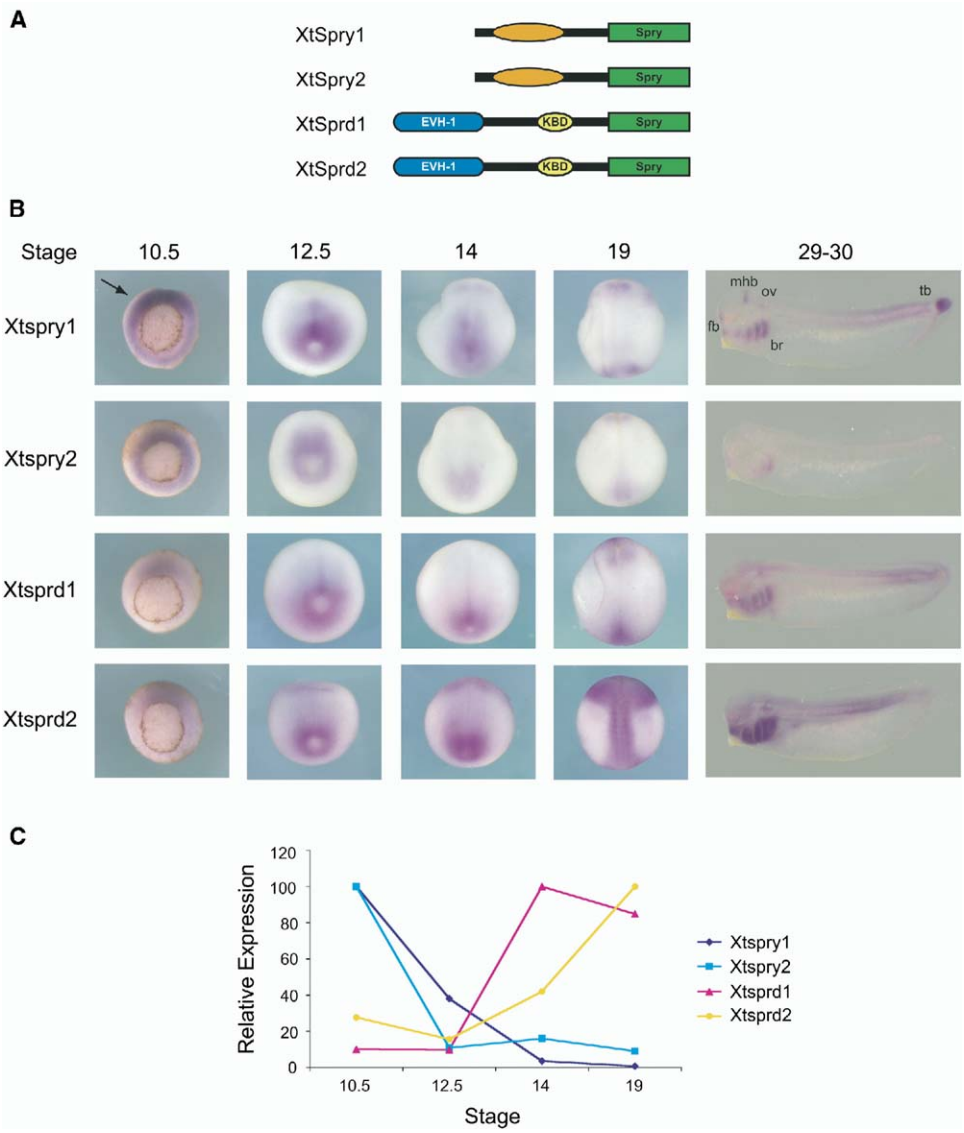

Figure 2. *Xtsproutys* and *Xtspreds* Are Expressed in Similar Patterns, but at Slightly Different Times

(A) Cartoon depiction of domain structures for each protein. Spry, conserved Sprouty domain; EVH-1, VASP homology domain; KBD, c-Kit binding domain.

(B) In situ hybridizations for each gene. At gastrula stages (stage 10.5), *Xtsproutys* showed more extensive staining around the blastopore than *Xtspreds* (arrow). Neurula stages showed increased staining of *Xtspreds* and decreased *Xtsproutys*. Tail bud stages showed similar staining in branchial arches (br), otic vesicle (ov), and tail bud (tb), but *Xtspred* staining was absent in mid-brain/hind-brain isthmus (mhb) and forebrain (fb).

(C) Quantitative real-time RT-PCR analysis of each gene's expression over time. Relative expression levels showed *Xtsproutys* peak before stage 12.5 and then diminish, while *Xtspreds* levels increased after stage 12.5.

on MAPK activity. However, both XtSpred proteins blocked MAPK signaling as efficiently as the dominant-negative FGF receptor (XFD) (Figure 3D). Since Sprouty proteins have been studied as inhibitors of the MAPK signaling pathway in vitro, we tested the possibility that the XtSproutys might be more effective at inhibiting MAPK activation at higher concentrations. A dosage series with the most effective family member, *Xtspry2*, was able to slightly reduce MAPK activation at the highest amount tested (2 ng), but *Xtsprd1* completely abolished MAPK activation even at 1 ng (Figure 3E). This suggests that the XtSpred proteins are much more effective inhibitors of MAPK signaling than the XtSprouty proteins in vivo. Others have similarly reported that mammalian Spred proteins are more effective MAPK inhibitors than the Sprouty proteins (Wakioka et al., 2001).

We also tested the effect of FGF-induced MAPK activation in animal caps. Compared to the results in Figure 3D, which tested steady state MAPK activity in whole embryos, this experiment directly tested the FGF-dependent activation of MAPK in animal caps after 15

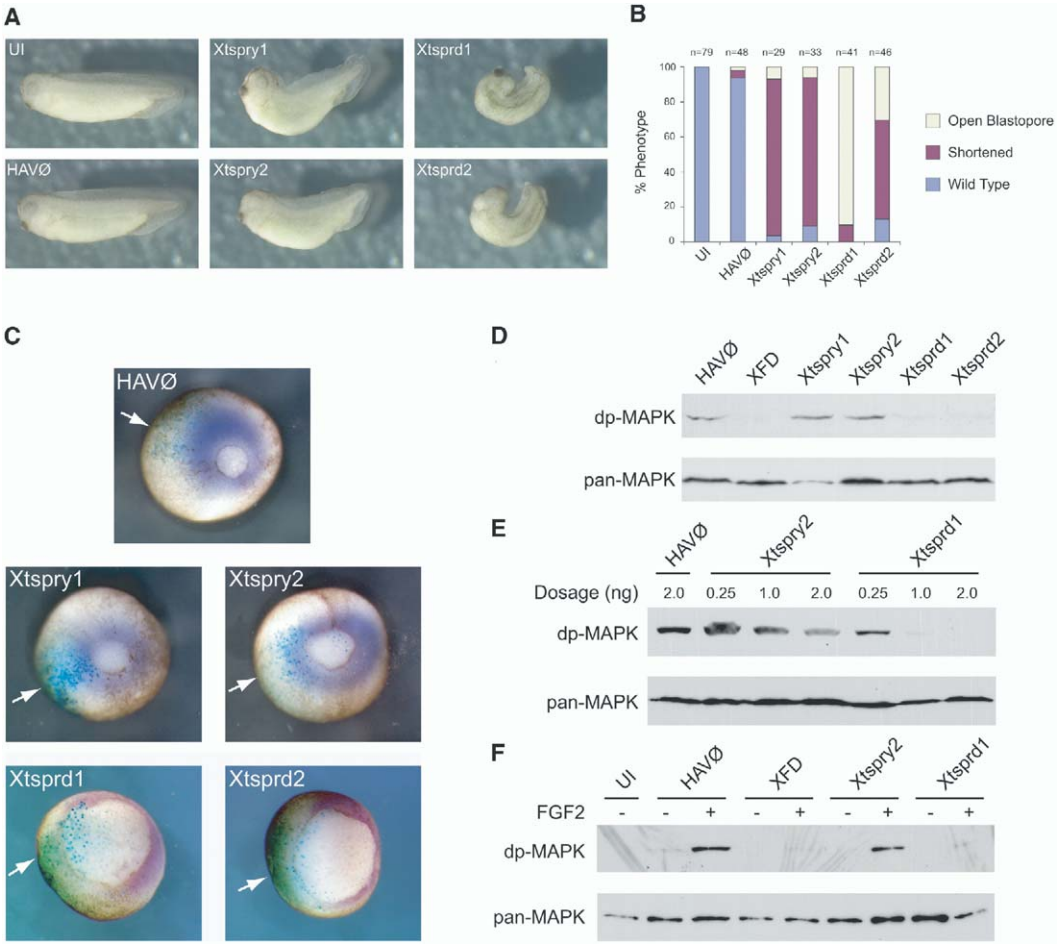

Figure 3. *Xtsprouty* and *Xtspred* Misexpressions Cause Distinct Phenotypes

(A) Stage 33–34 embryos after injection with 1 ng of indicated RNAs at the two-cell stage in the dorsal marginal zone. *Xtspry1*- and *Xtspry2*-injected embryos displayed a shortened A-P axis, while *Xtsprd1*- and *Xtsprd2*-injected embryos developed an open blastopore.

(B) Quantification of overexpression phenotypes, sorted into wild-type, shortened, and open blastopore categories.

(C) Embryos coinjected with RNAs and β-gal into one blastomere at the two-cell stage. X-gal staining (blue, arrows) and in situ hybridization for *Xbra* (purple) at the mid-gastrula (stage 11) showed that both *Xtsprd1* and *Xtsprd2* blocked *Xbra* expression but *Xtspry1* and *Xtspry2* had little effect.

(D) Western blots of lysates from stage 11 embryos injected into both blastomeres and probed for dp-MAPK or pan-MAPK. HAVØ control showed a dp-MAPK band that was blocked by XtSprd1, XtSprd2, and dnFGFR (XFD). XtSpry1 and XtSpry2 had no effect on MAPK activation.

(E) Dosage series of lysates from stage 11 embryos injected as above with 0.25, 1.0, and 2.0 ng RNAs. XtSprd1 was much more effective than XtSpry2 at reducing dp-MAPK signal.

(F) Blot of animal cap lysates cultured with and without FGF2 for 15 min and then probed for dp-MAPK. HAVØ control showed an increase of dp-MAPK when FGF2 treated. This signal was absent from caps injected with *Xtsprd1* and XFD, but not from caps injected with *Xtspry2*. UI, uninjected embryo; HAVØ, control RNA; XFD, dominant-negative FGFR.

min. As expected, untreated caps did not contain activated MAPK. Addition of FGF2 to control-injected caps led to a clear increase in activated MAPK, which was blocked by injection of dnFGFR (XFD). MAPK activation was largely unaffected by injection of 1.0 ng *Xtspry2* RNA but was blocked by *Xtsprd1* (Figure 3F).

XtSproutys Inhibit Morphogenesis Independently of Mesoderm Specification

We tested the effects of the *Xtsproutys* and *Xtspreds* on morphogenesis using an animal cap assay. Animal caps were dissected from injected embryos and cultured in the presence or absence of activin. Under activin treatment, control caps express mesodermal markers and undergo FGF-dependent convergent extension movements (Cornell and Kimelman, 1994). In this experiment the most effective members of each family, *Xtspry2* and *Xtsprd1*, were injected into animal poles. Each resulted in inhibition of cap extension in the presence of activin (Figure 4A). In light of the phenotypic differences we had observed, we wondered whether the inhibition of cap extension was due to the same underlying factors. RT-PCR was performed on gastrula (stage 11) caps injected as above with primers amplifying the mesodermal marker *Xbra* (Figure 4B). As expected, HAVØ control caps showed little *Xbra* expres-

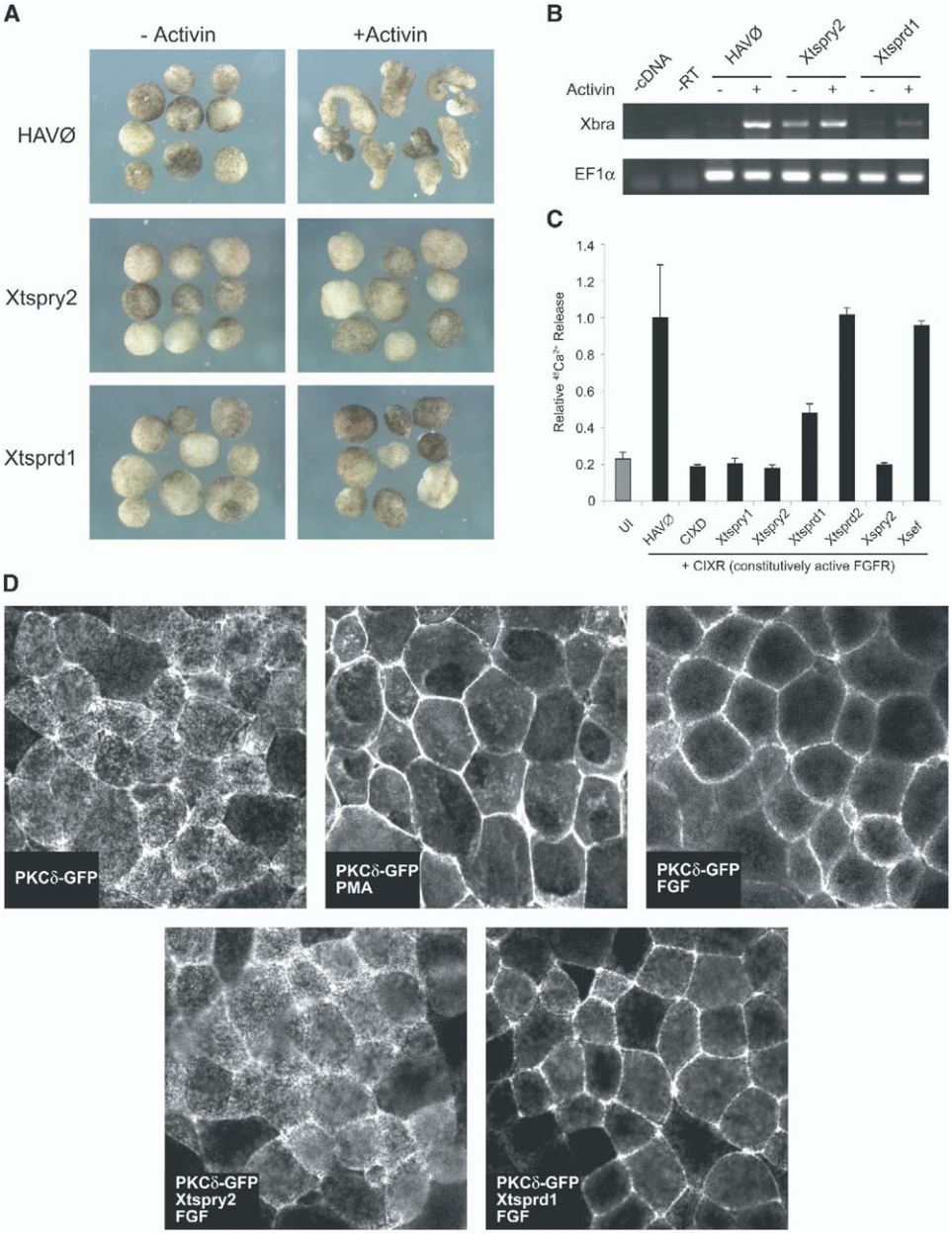

Figure 4. XtSproutys Inhibit Morphogenesis and FGF-Induced Ca^{2+} and PKCδ Signaling

(A) Animal caps cultured with and without activin until mid-neurula stages. Caps injected with HAVØ control extended when treated with activin, but *Xtspry2*- or *Xtsprd1*-injected caps did not.

(B) RT-PCR results from stage 11 animal caps injected as above. Activin treatment increased *Xbra* expression in HAVØ controls. *Xtspry2* increased *Xbra* expression in untreated caps, but had no effect after activin treatment. *Xtsprd1* inhibited *Xbra* expression with activin.

(C) Oocyte assay of Ca^{2+} signaling. Release of $^{45}Ca^{2+}$ from oocytes coinjected with constitutively active FGFR (CIXR) and the indicated RNAs was counted after 10 min. Addition of CIXR increased $^{45}Ca^{2+}$ release 5-fold (HAVØ). Coexpression of dominant-negative CIXR (CIXD), *Xtspry1*, *Xtspry2*, or *X. laevis Sprouty2* (*Xspry2*) effectively blocked this increase. *Xtsprd1* had significantly less effect, and *Xtsprd2* and *Xtsef* had no effect. Error bars represent standard deviation.

(D) Confocal images of PKCδ-GFP expressed in animal caps and cultured for 10 min in the presence of either 1 M PMA, 100 ng/ml FGF2, or coexpressed XtSpry2 or XtSprd1 as indicated. PKCδ was activated by both PMA and FGF2 and localized to the membrane. XtSpry2 inhibited FGF-induced localization of PKCδ but XtSprd1 did not.

sion unless treated with activin to induce mesoderm. *Xtspry2* had no effect on *Xbra* induction with activin, and surprisingly caused an increase in *Xbra* expression in the absence of activin. In comparison, injection of *Xtsprd1* inhibited the induction of *Xbra* after activin treatment. Therefore, morphogenetic extension was

blocked in *Xtspry2*- injected caps even though they still contained mesoderm, while the *Xtsprd1*-injected caps did not extend, but also lacked mesoderm.

XtSproutys Are More Effective Inhibitors of Ca^{2+} Signaling than XtSpreds

The MAPK cascade is only one of several signaling pathways that can be induced following FGFR activation. Another prominent downstream pathway acts through phospholipase Cγ (PLCγ). PLCγ hydrolyzes phosphatidylinositol into diacylglycerol (DAG) and inositol trisphosphate (IP_3), which activates the IP_3 receptor in the endoplasmic reticulum, causing an efflux of Ca^{2+} into the cytoplasm (Schlessinger, 2000). Localized Ca^{2+} signaling has been linked to convergent extension movements during *Xenopus* gastrulation (Wallingford et al., 2001). We have previously reported that *X. laevis* Sprouty2 inhibits FGF-induced Ca^{2+} mobilization in an efflux assay using *Xenopus* oocytes (Nutt et al., 2001). Using the same assay we compared the effect of the XtSprouty and XtSpred proteins on FGFR-induced Ca^{2+} release. Both XtSpry1 and XtSpry2 were as effective as *X. laevis* Spry2 in blocking Ca^{2+} release (Figure 4C). In contrast, XtSprd1 only partially inhibited Ca^{2+} release and XtSprd2 was ineffective. A negative control was provided by XtSef, an inhibitor of FGFR signaling that targets the Ras/MAPK pathway and bears no homology to the Sprouty family (Furthauer et al., 2002). These results provide additional evidence that XtSprouty and XtSpred proteins target different signaling pathways downstream of FGFR activation.

FGF-Induced PKCδ Localization Is Inhibited by XtSproutys but Not by XtSpreds

Another important secondary messenger produced by PLCγ in addition to IP_3 is DAG. The most prominent intracellular targets of DAG belong to the protein kinase C (PKC) family. Kinoshita et al. (2003) recently demonstrated that upon activation, PKCδ, a member of the novel (nPKC) subfamily, translocates to the cell membrane where it is an essential component of the noncanonical Wnt, or planar cell polarity, signaling pathway. Inhibition of PKCδ disrupts convergent extension movements during gastrulation, but does not block the expression of mesodermal markers (Kinoshita et al., 2003). Given the similarities of these results to our observations with XtSproutys, and that nPKC proteins rely solely on DAG for activation (Gschwendt, 1999), we tested whether FGFR signaling can activate PKCδ.

Membrane localization of GFP-tagged PKCδ was observed in animal caps using confocal microscopy (Figure 4D). PKCδ-GFP signal was diffuse in untreated caps, but addition of phorbol 12-myristate 13-acetate (PMA), a DAG analog, caused its translocation to cell membranes. Interestingly, addition of FGF2 also caused PKCδ-GFP to localize to the membrane. This localization was inhibited if XtSpry2 was coexpressed with PKCδ-GFP, but not when coexpressed with XtSprd1 (Figure 4D). These results provide additional evidence that XtSproutys target a distinct PLCγ-mediated signaling pathway compared with XtSpreds downstream of the FGFR.

Loss of XtSprouty and XtSpred Functions Causes Distinct Phenotypes

Loss-of-function experiments were conducted for XtSprouty and XtSpred proteins using antisense morpholino oligonucleotides (MOs). We have previously used this technique to effectively abrogate RNA translation and/or splicing by injecting MOs directly into early embryos (Kenwrick et al., 2004). MO sequences were designed to specifically target splice junctions for each *Xtsprouty* and *Xtspred* pre-mRNA. A cartoon depicting the design and targeting of splice morpholinos is shown in Figure 5A. Each MO sequence was designated by its target location (e.g., e1i1 for the exon1-intron1 boundary, i1e2 for the intron1-exon2 boundary, etc.). We confirmed the effectiveness of the morpholinos by assaying for splicing interference by performing RT-PCR using primers across each splice junction. Affected transcripts either amplified at different sizes or failed to amplify (Figure 5B).

X. tropicalis embryos were used for these experiments as their diploid genome allows for much simpler loss-of-function interpretation than the allotetraploid *X. laevis*. In each experiment, MOs were injected into zygotes before first cleavage. As a control, a MO containing four mismatches to the Xtspry2 sequence (4-mis) was used. Injection of MOs targeted to the *Xtsprouty* and *Xtspred* genes developed markedly different phenotypes (Figures 5C and 5E). In these experiments, combinations of splice MOs were used in order to reduce the effects of functional redundancy between family members. A combination of *Xtspry1* and *Xtspry2* MOs (Spry1 i1e2 and Spry2 e1i1) caused anterior-posterior truncations. These results were similar to the gain-of-function effect (Figure 3A), which might be expected if coordination of morphogenesis was disrupted. In contrast, MOs targeting the *Xtspred* genes (using a combination of Sprd1 e1i1 and Sprd2 e2i2 MOs) produced a more severe phenotype, with embryos appearing ventro-posteriorized (Figures 5C and 5E). This effect is reminiscent of that reported for embryos with overactive FGFR signaling (Isaacs et al., 1994). *Xtsprd* MO-injected embryos had diffuse and weak *cardiac actin* staining and had either absent or undifferentiated notochords (Figures 5C and 5D). Similarly, *Xtsprd* MO embryos showed no staining for the notochord marker *FK506 binding protein* (Spokony and Saint-Jeannet, 2000) (Figures 5E and 5F). In contrast, *Xtspry* MO-injected embryos stained normally for *cardiac actin* expression and the notochord was clearly visible (Figures 5C–5F).

XtSprouty Depletion Causes Animal Caps to Undergo Morphogenetic Extension, while XtSpred Depletion Inhibits Extension

Animal caps isolated from MO-injected embryos were incubated with and without activin (10 ng/ml) and assayed for extension. Both uninjected and 4-mis-injected caps remained as rounded balls when left untreated but elongated in the presence of activin (Figure 6A). However, animal caps isolated from *Xtsprouty* and *Xtspred* depleted embryos had strikingly different outcomes. Caps injected with combined Spry1 and Spry2 splice MOs

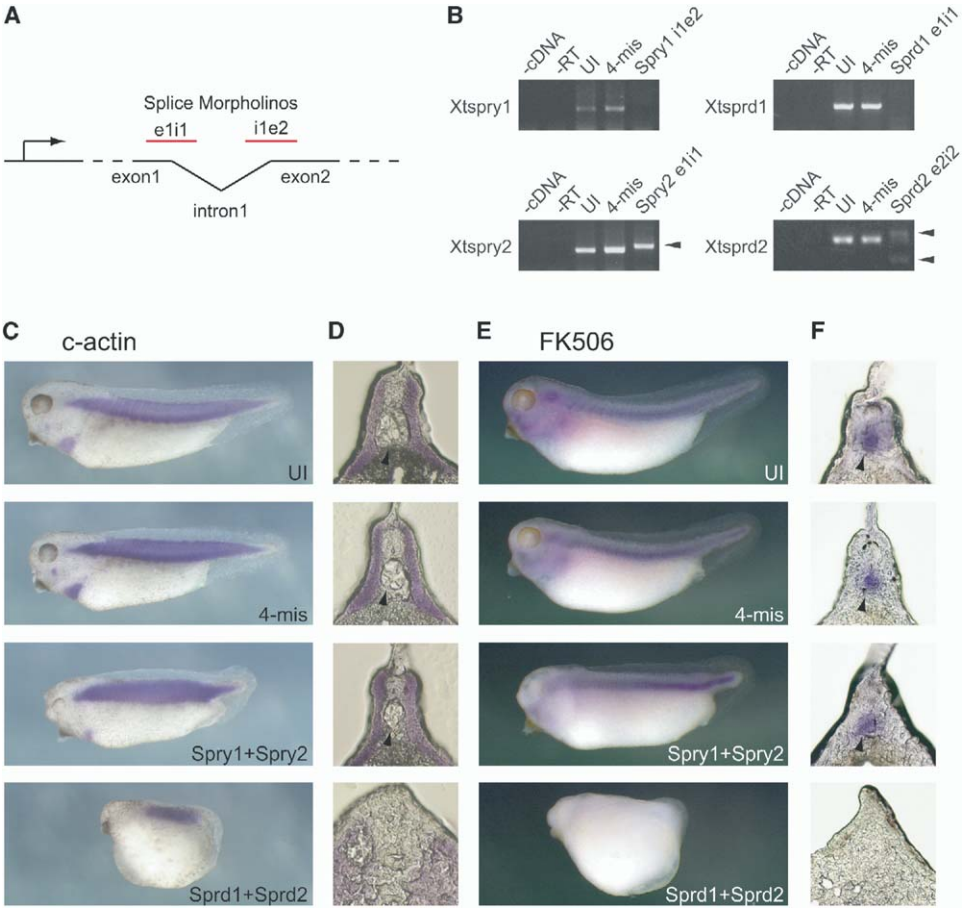

Figure 5. Loss of *Xtsprouty* and *Xtspred* Functions Causes Distinct Phenotypes

(A) Cartoon depicting splice MO designs at either end of splice junctions.

(B) RT-PCRs of MO-injected embryos. MO-injected lanes show bands either absent or shifted (arrowheads).

(C and E) Embryos injected with MOs before first cleavage assayed for *cardiac actin* and *FK506bp* expression at stage 35 by in situ hybridization (purple). Embryos injected with 4-mis control MOs appeared identical to uninjected embryos (UI). Injection of combined Spry1 and Spry2 MOs (Spry 1+2) produced a truncated phenotype, while injection of Sprd1 and Sprd2 MOs (Sprd 1+2) produced a severe ventroposteriorized phenotype.

(D and F) Corresponding crosssections through trunks of embryos injected as above. Spry MO embryos appeared relatively normal in crosssection, but Sprd MO embryos showed disrupted somites and absence of a notochord (arrowhead).

elongated in the *absence* of activin, but Sprd1 and Sprd2 splice MO caps failed to extend significantly in the *presence* of activin (Figure 6A). In order to confirm that we had specifically reduced XtSprouty and XtSpred protein function, we designed another set of MOs to these genes, targeting the start ATGs of each mRNA to inhibit translation. Similar to splice MOs, injection of Spry2 ATG MOs also induced cap extension in the absence of activin, while Sprd1 ATG MOs inhibited extension with activin (Figures 6B and 6C). Therefore, two different MOs targeting separate regions of the mRNAs caused the same phenotypes, confirming the specificity of the experiments. The resulting animal cap extensions of MO-injected embryos are summarized in Figure 6C.

Extension of animal caps in the absence of activin was an unexpected and unusual result. We wondered whether the XtSprouty depleted animal caps also developed mesoderm in the absence of activin. Therefore, expression of mesodermal markers was checked in animal caps at mid-gastrula stages by RT-PCR. In the absence of activin, both uninjected and 4-mis-injected embryos expressed a small amount of *Xtbra, Xtwnt11*, and *Xtwnt8* message (Figure 6D). This amount is not enough to convert the tissue to mesoderm. Although animal caps depleted for XtSproutys elongated, they had little increase in the expression of these early mesoderm markers. Therefore, loss of XtSprouty function allowed morphogenetic movements to occur without a significant increase in mesoderm specification. Conversely, XtSpred depleted animal caps exhibited a significant increase in the expression of these mesoderm markers in the absence of activin, but did not extend. Therefore, loss of XtSpred function allowed an increase in mesoderm specification without induction of morphogenetic movements. Taken together, these re-

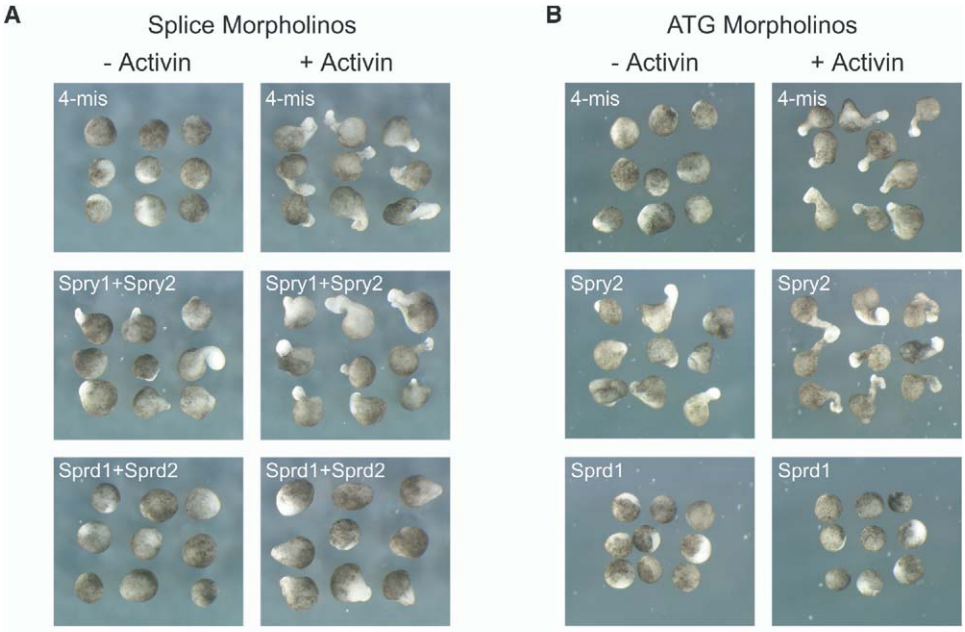

C

Injection/Treatment	% Extension -	+	++	*n*
UI -activin	100	0	0	35
UI +activin	6	23	71	31
4-mis -activin	96	4	0	44
4-mis +activin	8	15	77	47
Splice Morpholinos				
Spry1+Spry2 -activin	17	44	39	18
Spry1+Spry2 +activin	5	6	89	19
Sprd1+Sprd2 -activin	100	0	0	16
Sprd1+Sprd2 +activin	60	40	0	15
ATG Morpholinos				
Spry2 -activin	16	21	63	24
Spry2 +activin	14	14	72	29
Sprd1 -activin	100	0	0	26
Sprd1 +activin	84	16	0	31

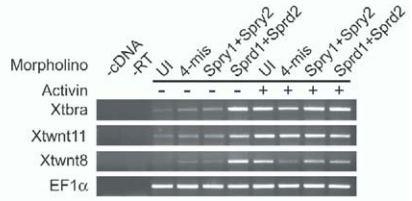

Figure 6. XtSprouty Depletion Causes Animal Caps To Extend, but XtSpred Depletion Inhibits Cap Extension

(A) Animal cap assays with and without activin treatment following MO injection. 4-mis control-injected caps extended after activin treatment. Combined XtSprouty1+2 splice MO-injected caps extended in the absence of activin, while XtSpred1+2 splice MO-injected caps were inhibited from extending after activin treatment.

(B) Assays as above using ATG MOs showed similar results to splice MOs.

(C) Summary of animal cap extension results indicating percent of caps remaining round (-), starting to extend (+), and clearly extended (++).

(D) RT-PCR results for *Xtbra, Xtwnt11, Xtwnt8*, and *EF1*α expression in MO-injected caps with and without activin. Caps injected with Spred MOs strongly expressed these mesodermal markers even when untreated, but Spry MOs had little effect on the expression of these markers.

sults support the differences observed from mis-expression experiments: XtSproutys inhibit a branch of FGFR signaling that regulates morphogenesis, while the XtSpreds regulate mesoderm specification.

Discussion

In recent years, it has become apparent that a great variety of developmental decisions are controlled by only a handful of morphogenic signals. For example, RTK activation by the FGF family of secreted factors has been implicated in cell differentiation, growth, migration, wound healing, and angiogenesis (Robertson et al., 2000; Schlessinger, 2000; Sivak and Amaya, 2004). In some cases FGFs are used for multiple decisions at essentially the same time (Sivak and Amaya, 2004). Therefore, an important question arises: how can the same signal be interpreted as performing different

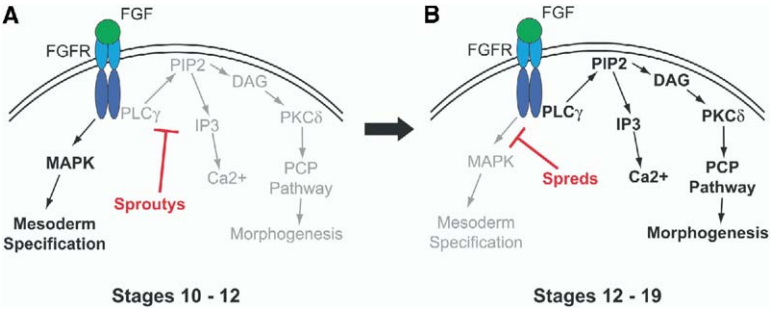

Figure 7. Model of Sprouty and Spred Regulated Switching of FGFR Signal Pathways

(A) *Xtsproutys* are expressed first, resulting in inhibition of the PLCγ/morphogenesis pathway downstream of the FGFR while the MAPK/mesoderm specification pathway proceeds.

(B) As mesoderm specification finishes, *Xtspred* expression increases, resulting in inhibition of the mesoderm specification pathway. At this point expression of *Xtsproutys* diminishes, allowing the morphogenesis pathway to proceed.

functions, often within the same cells? The related Sprouty and Spred families are recently discovered proteins that function to directly regulate RTK signaling downstream of receptor activation (Christofori, 2003; Guy et al., 2003). Here we have described divergent roles for Sproutys and Spreds in regulation of FGFR signaling during vertebrate gastrulation: XtSprouty proteins inhibit morphogenesis, PKCδ activation, and Ca^{2+} signaling, and XtSpreds inhibit mesoderm specification and MAPK activation. In this manner XtSproutys and XtSpreds can switch between activation of two FGFR signal pathways to coordinate distinct developmental events.

Functional Divergence of Xtsprouty and Xtspred Proteins

Gain- and loss-of-function experiments revealed marked differences between XtSprouty and XtSpred functions in vivo. *Xtsprouty* misexpression resulted in shortened embryos and inhibited morphogenic movements but left mesoderm formation intact. FGFR-dependent MAPK activation was only weakly affected, but PKCδ activation and Ca^{2+} signaling were strongly inhibited. Notably, *Xbra* was induced in untreated animal caps overexpressing *Xtspry2*, suggesting that in this context XtSprouty proteins can actually enhance the mesoderm specification pathway. Conversely, XtSprouty depletion caused untreated animal caps to undergo morphogenetic extensions without an accompanying increase in mesoderm. This striking result is similar to the one observed when an activated version of protein-tyrosine phosphatase SHP-2 is missexpressed in animal caps (O'Reilly et al., 2000). Interestingly, this same activated version of SHP-2 has recently been shown to dephosphorylate and inactivate Sprouty (Hanafusa et al., 2004). Therefore, it may be possible that untreated animal caps expressing activated SHP-2 elongate because Sprouty is inactivated, a question that is now being investigated.

In other model systems Sproutys have also consistently been associated with morphogenesis and cell migration, processes not normally associated with MAPK signaling (Lim et al., 2000; Yigzaw et al., 2001, 2003). In particular, depletion of Sproutys has been reported to cause excessive morphogenesis in mice and flies (Hacohen et al., 1998; Tefft et al., 1999). The animal cap extensions we observed after XtSprouty depletion is reminiscent of these other cases. We have shown here that XtSproutys are efficient inhibitors of FGFR-dependent Ca^{2+} signaling and PKCδ activation, two major outcomes of PLCγ activation. Importantly, PKCδ has recently been demonstrated to be an essential component of the wnt/planar cell polarity pathway involved in regulating morphogenesis (Kinoshita et al., 2003). Ca^{2+} signaling has also been implicated in control of convergent extension movements without affecting cell fate (Wallingford et al., 2001). Therefore, these results provide evidence of a mechanism directly linking FGFR signaling to cell migration/cell polarity pathways.

In contrast, XtSpreds inhibited mesoderm differentiation through strong inhibition of MAPK activation and had little effect on Ca^{2+} signaling or PKCδ activation. Embryos injected with *Xtspred1* and *Xtspred2* RNAs did not develop mesoderm and displayed an open blastopore phenotype reminiscent of the effect of dnFGFR (Amaya et al., 1991). Likewise, XtSpred proteins blocked MAPK activity and extension in animal caps. These results are consistent with studies showing that mammalian Spreds inhibit Raf activation upstream of MAPK (Kato et al., 2003; Wakioka et al., 2001). Interestingly, the timing of expression of the *Xtspred* genes correlates with the loss of MAPK activity in embryos, suggesting that the decrease in MAPK activity is due to the expression of the *Xtspred* genes. Depletion of XtSpreds resulted in ventro-posteriorized embryos that lacked a notochord, similar to the effect of constitutive FGFR signaling (Isaacs et al., 1994). Loss of XtSpreds in animal caps inhibited elongations with activin treatment. However, increased mesoderm was detected in untreated *Xtspred*-depleted caps, indicating excessive mesoderm formation consistent with XtSpreds acting as MAPK inhibitors.

Taken together, these results describe a molecular branching of FGFR signaling during mesoderm formation and morphogenesis: a Sprouty-sensitive pathway affecting PKCδ activation and Ca^{2+} signaling and mediating morphogenesis, and a Spred-sensitive pathway affecting MAPK activity and mesoderm specification. With the identification of these two regulatory pathways it will now be possible to dissect the various downstream elements involved in each branch. One important aspect to address will be the functional roles contributed by the various XtSprouty and XtSpred protein domains in order to identify the elements regulating their specificity. As there is considerable divergence between *Drosophila* and vertebrate Sprouty sequences, Sprouty and Spred functions may have become specialized to accomplish specific signaling tasks during vertebrate evolution.

A Switching Mechanism for FGFR Signal Interpretation

FGFR-dependent activation of the Ras/MAPK pathway is necessary for specification of mesoderm in vivo (Sivak and Amaya, 2004). However, we have demonstrated a role for FGFR signaling in the morphogenetic cell movements that follow as well. Several other studies have also demonstrated a role of FGFR signaling in morphogenesis during gastrulation (Ciruna and Rossant, 2001; Nutt et al., 2001; Yang et al., 2002). Notably, we have shown here that although FGFR function is required, MAPK is not active during the majority of morphogenesis in the early embryo. Therefore a developmental switch to a different FGFR signaling pathway must be made to mediate this function.

All four *Xtsproutys* and *Xtspreds* analyzed had largely overlapping expression patterns. However, we found variations over time, which has important implications for the regulation of FGFR signaling. Expression of *Xtspry1* and *2* are relatively stronger during early gastrulation, peaking by stage 10.5, after which expression levels are reduced. In contrast, *Xtsprd1* and *2* are expressed at lower levels during early gastrulation but rise after stage 12, when morphogenesis predominates. When these temporal differences are compared with the signaling pathways targeted by each gene family, a model of FGFR signal switching can be proposed (Figure 7).

During the early stages of gastrulation, FGFR signaling is necessary to maintain specification of mesodermal tissues. At this time, *Xtsproutys* are strongly expressed and inhibit the PLCγ pathway regulating morphogenetic movements. Consequently, the predominant signal transduced downstream of the FGFR is the ras/MAPK pathway, leading to transcription of mesodermal genes such as *Xbra*. As gastrulation proceeds, *Xtsprouty* transcription decreases and *Xtspred* transcription increases. As a result, the ras/MAPK pathway is inhibited and the predominant pathway is switched toward regulation of morphogenesis. A key advantage of this mechanism is that FGF signal interpretation occurs relatively quickly at the cell membrane to allow for plastic and responsive changes to events during a rapid early developmental timescale. However, this model may be complicated by positive and/or negative feedback due to the fact that Sproutys, and likely Spreds, are themselves downstream targets of FGFR signaling (Minowada et al., 1999; Nutt et al., 2001).

In conclusion, we have uncovered consistent functional differences between XtSprouty and XtSpred proteins downstream of the FGFR that are used to coordinate FGF signal interpretation during vertebrate morphogenesis. It will be interesting to discover if similar mechanisms are involved in regulating other examples of RTK activity.

Experimental Procedures

Isolation of *Xtsprouty* and *Xtspred* Genes and Construct Design

X. tropicalis Sprouty-related homologs were identified through searches of the Wellcome Trust Full Length Database against human and *X. laevis* EST sequences. Four genes were identified: *Xtsprouty1* (*Xtspry1*; clone TNeu048o16), *Xtsprouty2* (*Xtspry2*; TGas112n24), *Xtspred1* (*Xtsprd1*; TNeu018m17), and *Xtspred2* (*Xtsprd2*; TGas019j20). Full-length clones were purified from corresponding EST libraries (Gilchrist et al., 2004). In some cases extraneous sequence was deleted to remove unwanted regulatory elements. The *Xtspry1* clone TGas112n24 was missing 86 bases of coding sequence at the 5′ end, which was replaced by searching the JGI *X. tropicalis* Genomic Database to identify the corresponding sequence. GenBank accession numbers are as follows: *Xtspry1*, AY714335; *Xtspry2*, AY714336; *Xtsprd1*, AY714338; *Xtsprd2*, AY714337). In situ hybridizations were performed according to established protocols using antisense DIG-labeled probes.

Dominant-negative FGF receptor (XFD), nonfunctional FGF receptor (HAVϕ), constitutively active FGFR1 (pCIXR), and its corresponding dominant-negative (pCIXD) have been previously described (Amaya et al., 1991; Nutt et al., 2001). Full-length *X. laevis* PKCδ1 was obtained from the I.M.A.G.E. Consortium (Invitrogen/Resgen, 4969220) and subcloned into the StuI and XhoI sites of the pCSGFP3-TAA vector to generate an N-terminal PKCδ-GFP fusion.

RNA Synthesis and Embryo Microinjections

Capped mRNA was synthesized using the mMessage Machine kit according to the manufacturer's directions (Ambion). Embryos were cultured and injected with RNAs according to established protocol. Developmental staging was assessed as described (Nieuwkoop and Faber, 1967). Generally, 100 pg of nuclear localized β-galactosidase (pnucβ-gal) or GFP RNA were coinjected as a lineage tracer. For animal cap experiments, embryos were injected at animal poles and cap tissue was excised at stage 8. Caps were then incubated in either 0.4× MMR (for extension experiments) or 1× MMR (for MAPK assay). Human recombinant activin A (R&D Systems) was added at 10 ng/ml, and FGF2 (a gift of Dr. Harry Isaacs) was added at 100 ng/ml.

FGFR and MAPK Inhibitor Treatments

Embryos were cultured to stage 8 or 12.5 and injected into the blastocoel with 10 nl of a 2 mM DMSO stock of either SU5402 (Calbiochem), an FGFR1 kinase activity inhibitor, or U0126 (Calbiochem), a MEK1 inhibitor, and cultured in 0.1× MMR with 20 μM of the corresponding inhibitor. Embryos treated at stage 8 were fixed at stages 11.5 and 29–30 for in situ hybridization. Embryos treated at stage 12.5 were fixed at stage 31 and photographed.

Cellular Localization Assay

100 pg PKCδ-GFP mRNA was coinjected into *X. laevis* animal poles with *Xtspry2* or *Xtsprd1.* Animal caps were excised at stage 9 in 1× modified Danilchik's medium (DFA) to prevent healing (Sater et al., 1994) and were cultured for 10 min in 1× DFA with or without 100 ng/ml FGF2 or 1 μM PMA (Sigma). Caps were lightly fixed in formaldehyde for 20 min and GFP localization was determined by confocal microscopy.

Morpholino Design and Microinjections

MOs were purchased from Gene Tools LLC. RNA splice junctions were identified by alignment of cDNA sequences with matching genomic sequences. *X. tropicalis* embryos were injected with 10 ng total MOs before first cleavage, and were generally coinjected with a fluorescent control MO (Li std; Gene Tools). MO sequences are listed as follows. ATG MOs: 4-mis Spry2, 5′-GCC**TTTT**AG TACTCTCGT**G**TCC**T**TC-3′ (mismatch bases are bold); Spry2 ATG, 5′-GCCATTTTGTACTCTCGTCTCCATC-3′; Sprd1 ATG, 5′-CCTGTT CGCCGCTCATTGTCCCCTT-3′; Sprd2 ATG, 5′-TCCTCGCTCATT TTGTCCCTGCTCA-3′; Splice MOs (intron sequences are lower case): Spry1 i1e2, 5′-CATCTGAAAACctgccgatcaaaac-3′; Spry2 e1i1, 5′- gtacttacCGTGACCTCCTCGCCCC-3′; Sprd1 e1i1, 5′-ggtg gcactcacTCTGGCTCCTGTT-3′; Sprd2 e2i2, 5′-ttccttaCCAGTTTG TCATTCAGTC-3′.

RNA Isolation and RT-PCR

Total RNA was isolated from embryos and animal caps using the TRIzol reagent according to manufacturer's instructions (Invitrogen). cDNA was synthesized using AMV reverse transcriptase (Roche), and PCR reactions were performed using *Taq* polymerase (Roche) according to established protocol. Primer sequences are

written 5′ to 3′ as follows. Xtspry1 forward, CGCAGTTCCGATCG GATTTGC; reverse, CACTATTTGTGCTACCAGAAC; Xtspry2 f, CAT GCGAATTCATGGAGACGAGAGTAC; r, GTGTGGCGTAGTCTGTCG TGG; Xtsprd1 f, CGCACTTCCCATATAACCTC; r, CCTGTGGTCCA TCCTCAGAAG; Xtsprd2 f, GACGGTCCTCTTCGATGCTGC; r, CCA AGCTCTGCCTCATTATGG; Xbra f, AGACATCTTGGATGAGGG; r, GAAGGGTACTGACTTGAG. Xtwnt11 f, TACTCATCTTGTGCTGCTC CAGG; r, ACAAGCACGAGCAATGGTATGG; Xtwnt8 f, CTGAAGATC AAGCACGACCA; r, CAGCTCCTTCTTTCCCACTG. Control primers for EF1α (Hemmati-Brivanlou and Melton, 1994) and ornithine decarboxylase (ODC) (Heasman et al., 2000) have been previously described. Real-time RT-PCR analysis was performed using a Light-Cycler System™ (Roche).

$^{45}Ca^{2+}$ Efflux Assay

Oocytes were isolated, injected, and cultured for 48 hr in modified Barth's saline (MBSH) at 16°C and then assayed for $^{45}Ca^{2+}$ efflux as described (Musci et al., 1990). 10 ng of each RNA was injected along with 1 ng of pCIXR, a constitutively active FGF receptor (Nutt et al., 2001).

Immunoblotting

For assays of MAPK activity, 10 embryos or animal caps were homogenized in 1× RIPA lysis buffer with the addition of Complete protease inhibitor cocktail (Roche) and 50 mM sodium fluoride and 10 mM sodium orthovanadate to inhibit phosphatase activity. In whole embryos, freon was used to extract yolk proteins according to established protocol. Western blots were probed with 1:10000 mouse anti-dpMAPK (clone MAPK-YT, Sigma) or 1:2000 mouse anti-panMAPK (Clone 16, Transduction Laboratories) according to established protocols.

Acknowledgments

The authors would like to acknowledge the advice and suggestions of Andrew Chalmers and Nancy Papalopulu. Also, thanks to Michael Gilchrist for constructing and maintaining the *X. tropicalis* EST database, and thanks to Jun-An Chen for providing the *X. tropicalis* FK506 clone. This work was funded by a Wellcome Trust Prize Studentship (L.F.P.) and a Wellcome Trust Senior Research Fellowship (E.A.).

Received: October 22, 2004
Revised: January 5, 2005
Accepted: February 28, 2005
Published: April 3, 2005

References

Amaya, E., Musci, T.J., and Kirschner, M.W. (1991). Expression of a dominant negative mutant of the FGF receptor disrupts mesoderm formation in Xenopus embryos. Cell *66*, 257–270.

Casci, T., Vinos, J., and Freeman, M. (1999). Sprouty, an intracellular inhibitor of Ras signaling. Cell *96*, 655–665.

Christen, B., and Slack, J.M. (1997). FGF-8 is associated with anteroposterior patterning and limb regeneration in Xenopus. Dev. Biol. *192*, 455–466.

Christofori, G. (2003). Split personalities: the agonistic antagonist Sprouty. Nat. Cell Biol. *5*, 377–379.

Ciruna, B., and Rossant, J. (2001). FGF signaling regulates mesoderm cell fate specification and morphogenetic movement at the primitive streak. Dev. Cell *1*, 37–49.

Ciruna, B.G., Schwartz, L., Harpal, K., Yamaguchi, T.P., and Rossant, J. (1997). Chimeric analysis of fibroblast growth factor receptor-1 (Fgfr1) function: a role for FGFR1 in morphogenetic movement through the primitive streak. Development *124*, 2829–2841.

Cornell, R.A., and Kimelman, D. (1994). Activin-mediated mesoderm induction requires FGF. Development *120*, 453–462.

Furthauer, M., Lin, W., Ang, S.L., Thisse, B., and Thisse, C. (2002). Sef is a feedback-induced antagonist of Ras/MAPK-mediated FGF signalling. Nat. Cell Biol. *4*, 170–174.

Gilchrist, M.J., Zorn, A.M., Voigt, J., Smith, J.C., Papalopulu, N., and Amaya, E. (2004). Defining a large set of full-length clones from a *Xenopus tropicalis* EST project. Dev. Biol. *271*, 498–516.

Gschwendt, M. (1999). Protein kinase C delta. Eur. J. Biochem. *259*, 555–564.

Gupta, R.W., and Mayer, B.J. (1998). Dominant-negative mutants of the SH2/SH3 adapters Nck and Grb2 inhibit MAP kinase activation and mesoderm-specific gene induction by eFGF in Xenopus. Oncogene *17*, 2155–2165.

Guy, G.R., Wong, E.S., Yusoff, P., Chandramouli, S., Lo, T.L., Lim, J., and Fong, C.W. (2003). Sprouty: how does the branch manager work? J. Cell Sci. *116*, 3061–3068.

Hacohen, N., Kramer, S., Sutherland, D., Hiromi, Y., and Krasnow, M.A. (1998). sprouty encodes a novel antagonist of FGF signaling that patterns apical branching of the Drosophila airways. Cell *92*, 253–263.

Hanafusa, H., Torii, S., Yasunaga, T., and Nishida, E. (2002). Sprouty1 and Sprouty2 provide a control mechanism for the Ras/MAPK signalling pathway. Nat. Cell Biol. *4*, 850–858.

Hanafusa, H., Torii, S., Yasunaga, T., Matsumoto, K., and Nishida, E. (2004). Shp2, an SH2-containing protein-tyrosine phosphatase, positively regulates receptor tyrosine kinase signaling by dephosphorylating and inactivating the inhibitor Sprouty. J. Biol. Chem. *279*, 22992–22995.

Harmer, N.J., Sivak, J.M., Amaya, E., and Blundell, T. (2005). 1.65 Å Crystal structure of the X. tropicalis Spred1 Enabled/Vasodilator-stimulated phosphoprotein homology-1 domain. FEBS Lett. *579*, 1161–1166.

Heasman, J., Kofron, M., and Wylie, C. (2000). Beta-catenin signaling activity dissected in the early Xenopus embryo: a novel antisense approach. Dev. Biol. *222*, 124–134.

Hemmati-Brivanlou, A., and Melton, D.A. (1994). Inhibition of activin receptor signaling promotes neuralization in Xenopus. Cell *77*, 273–281.

Isaacs, H.V., Pownall, M.E., and Slack, J.M. (1994). eFGF regulates Xbra expression during Xenopus gastrulation. EMBO J. *13*, 4469–4481.

Kato, R., Nonami, A., Taketomi, T., Wakioka, T., Kuroiwa, A., Matsuda, Y., and Yoshimura, A. (2003). Molecular cloning of mammalian Spred-3 which suppresses tyrosine kinase-mediated Erk activation. Biochem. Biophys. Res. Commun. *302*, 767–772.

Kenwrick, S., Amaya, E., and Papalopulu, N. (2004). Pilot morpholino screen in Xenopus tropicalis identifies a novel gene involved in head development. Dev. Dyn. *229*, 289–299.

Kinoshita, N., Iioka, H., Miyakoshi, A., and Ueno, N. (2003). PKC delta is essential for Dishevelled function in a noncanonical Wnt pathway that regulates Xenopus convergent extension movements. Genes Dev. *17*, 1663–1676.

Kroll, K.L., and Amaya, E. (1996). Transgenic Xenopus embryos from sperm nuclear transplantations reveal FGF signaling requirements during gastrulation. Development *122*, 3173–3183.

Lim, J., Wong, E.S., Ong, S.H., Yusoff, P., Low, B.C., and Guy, G.R. (2000). Sprouty proteins are targeted to membrane ruffles upon growth factor receptor tyrosine kinase activation. Identification of a novel translocation domain. J. Biol. Chem. *275*, 32837–32845.

MacNicol, A.M., Muslin, A.J., and Williams, L.T. (1993). Raf-1 kinase is essential for early Xenopus development and mediates the induction of mesoderm by FGF. Cell *73*, 571–583.

Minowada, G., Jarvis, L.A., Chi, C.L., Neubuser, A., Sun, X., Hacohen, N., Krasnow, M.A., and Martin, G.R. (1999). Vertebrate Sprouty genes are induced by FGF signaling and can cause chondrodysplasia when overexpressed. Development *126*, 4465–4475.

Musci, T.J., Amaya, E., and Kirschner, M.W. (1990). Regulation of the fibroblast growth factor receptor in early Xenopus embryos. Proc. Natl. Acad. Sci. USA *87*, 8365–8369.

Nieuwkoop, P.D., and Faber, J. (1967). Normal Table of Xenopus Laevis (Amsterdam: North-Holland).

Nutt, S.L., Dingwell, K.S., Holt, C.E., and Amaya, E. (2001). Xenopus Sprouty2 inhibits FGF-mediated gastrulation movements but does not affect mesoderm induction and patterning. Genes Dev. *15*, 1152–1166.

O'Reilly, A.M., Pluskey, S., Shoelson, S.E., and Neel, B.G. (2000). Activated mutants of SHP-2 preferentially induce elongation of Xenopus animal caps. Mol. Cell. Biol. *20*, 299–311.

Robertson, S.C., Tynan, J., and Donoghue, D.J. (2000). RTK mutations and human syndromes: when good receptors turn bad. Trends Genet. *16*, 368.

Sasaki, A., Taketomi, T., Wakioka, T., Kato, R., and Yoshimura, A. (2001). Identification of a dominant negative mutant of Sprouty that potentiates fibroblast growth factor- but not epidermal growth factor-induced ERK activation. J. Biol. Chem. *276*, 36804–36808.

Sater, A.K., Alderton, J.M., and Steinhardt, R.A. (1994). An increase in intracellular pH during neural induction in Xenopus. Development *120*, 433–442.

Schlessinger, J. (2000). Cell signaling by receptor tyrosine kinases. Cell *103*, 211–225.

Sivak, J.M., and Amaya, E. (2004). FGF signaling during gastrulation. In Gastrulation, C. Stern, ed. (Woodbury, NY: Cold Spring Harbor Laboratory Press), pp. 463–473.

Song, J., and Slack, J.M. (1996). XFGF-9: a new fibroblast growth factor from Xenopus embryos. Dev. Dyn. *206*, 427–436.

Spokony, R., and Saint-Jeannet, J.P. (2000). Xenopus FK 506-binding protein, a novel immunophilin expressed during early development. Mech. Dev. *94*, 205–208.

Tang, T.L., Freeman, R.M., Jr., O'Reilly, A.M., Neel, B.G., and Sokol, S.Y. (1995). The SH2-containing protein-tyrosine phosphatase SH-PTP2 is required upstream of MAP kinase for early Xenopus development. Cell *80*, 473–483.

Tefft, J.D., Lee, M., Smith, S., Leinwand, M., Zhao, J., Bringas, P., Jr., Crowe, D.L., and Warburton, D. (1999). Conserved function of mSpry-2, a murine homolog of Drosophila sprouty, which negatively modulates respiratory organogenesis. Curr. Biol. *9*, 219–222.

Wakioka, T., Sasaki, A., Kato, R., Shouda, T., Matsumoto, A., Miyoshi, K., Tsuneoka, M., Komiya, S., Baron, R., and Yoshimura, A. (2001). Spred is a Sprouty-related suppressor of Ras signalling. Nature *412*, 647–651.

Wallingford, J.B., Ewald, A.J., Harland, R.M., and Fraser, S.E. (2001). Calcium signaling during convergent extension in Xenopus. Curr. Biol. *11*, 652–661.

Whitman, M., and Melton, D.A. (1992). Involvement of p21ras in Xenopus mesoderm induction. Nature *357*, 252–254.

Wong, E.S., Fong, C.W., Lim, J., Yusoff, P., Low, B.C., Langdon, W.Y., and Guy, G.R. (2002). Sprouty2 attenuates epidermal growth factor receptor ubiquitylation and endocytosis, and consequently enhances Ras/ERK signalling. EMBO J. *21*, 4796–4808.

Yang, X., Dormann, D., Munsterberg, A.E., and Weijer, C.J. (2002). Cell movement patterns during gastrulation in the chick are controlled by positive and negative chemotaxis mediated by FGF4 and FGF8. Dev. Cell *3*, 425–437.

Yigzaw, Y., Cartin, L., Pierre, S., Scholich, K., and Patel, T.B. (2001). The C terminus of sprouty is important for modulation of cellular migration and proliferation. J. Biol. Chem. *276*, 22742–22747.

Yigzaw, Y., Poppleton, H.M., Sreejayan, N., Hassid, A., and Patel, T.B. (2003). Protein-tyrosine phosphatase-1B (PTP1B) mediates the anti-migratory actions of Sprouty. J. Biol. Chem. *278*, 284–288.

Yusoff, P., Lao, D.H., Ong, S.H., Wong, E.S., Lim, J., Lo, T.L., Leong, H.F., Fong, C.W., and Guy, G.R. (2002). Sprouty2 inhibits the Ras/MAP kinase pathway by inhibiting the activation of Raf. J. Biol. Chem. *277*, 3195–3201.